

Schottky Barrier Photodetectors Based on  $\text{Mg}_{0.40}\text{Zn}_{0.60}\text{O}$  Thin Films

Dayong Jiang, Chongxin Shan, Jiying Zhang,\* Youming Lu, Bin Yao, Dongxu Zhao, Zhenzhong Zhang, Xiwu Fan, and Dezhen Shen

*Key Laboratory of Excited State Processes, Changchun Institute of Optics, Fine Mechanics and Physics, Chinese Academy of Sciences, and Graduate School of the Chinese Academy of Sciences, Beijing 100049, China*

Received July 3, 2008; Revised Manuscript Received October 5, 2008

**ABSTRACT:** Wurtzite ( $\text{Mg}_{0.40}\text{Zn}_{0.60}\text{O}$ ) thin films have been grown on quartz substrates by using the radio frequency magnetron sputtering technique, and a metal–semiconductor–metal Schottky barrier photodetector has been fabricated from these films. The photodetector exhibits a peak responsivity at 276 nm and a very sharp cutoff wavelength at 295 nm corresponding to the absorption edge of the  $\text{Mg}_{0.40}\text{Zn}_{0.60}\text{O}$  thin film. At 2 V bias, the detectivity of the photodetector is  $1.1 \times 10^{12}$  (cm Hz<sup>1/2</sup>)/W at 276 nm, and the ultraviolet-to-visible rejection ratio [ $R(276 \text{ nm})/R(400 \text{ nm})$ ] is about 4 orders of magnitude. The photodetector also exhibits a very low dark current of about 100 pA at 2 V bias.

## Introduction

There is currently great interest in ultraviolet (UV) photodetectors due to their versatile applications, such as missile warning and tracking, engine/flame monitoring, chemical/biological agent detecting, and covert space-to-space communication, etc.<sup>1–4</sup>  $\text{Mg}_x\text{Zn}_{1-x}\text{O}$  has been considered as an ideal material for the UV photodetectors because it has high UV absorption coefficients and high visible transparency and it is abundant, inexpensive, and environmentally friendly as well. Ultraviolet band (UV-B) (280–320 nm) solar radiation has a huge effect on the earth ecosystem and human health.<sup>5</sup> The development of reliable and low-cost UV-B monitoring devices is thus an important issue. A  $\text{Mg}_x\text{Zn}_{1-x}\text{O}$ -based-photodetector, with a Mg mole fraction of about 0.4, is a very promising candidate for this UV-B detection, due to its suitable bandgap and superior radiation endurance.<sup>6–8</sup>

Many detailed studies on the growth of low-Mg-content (<20%)  $\text{Mg}_x\text{Zn}_{1-x}\text{O}$  photodetectors have been reported.<sup>9,10</sup> Yang et al. have demonstrated deep ultraviolet cubic  $\text{Mg}_x\text{Zn}_{1-x}\text{O}$  photodetectors, and the peak responsivity was at 225 nm, indicating that the Mg composition was about ~68%.<sup>11</sup> The main difficulty to be solved for devices based on a Mg component in the range from 37% to 62% is phase separation.<sup>11,12</sup> Furthermore, no Schottky barrier type photodetector based on  $\text{Mg}_x\text{Zn}_{1-x}\text{O}$  with high Mg content (>30%) has been reported to the best our knowledge, although this type can reduce the dark current and enlarge the ultraviolet-to-visible rejection. In this work, the Schottky barrier  $\text{Mg}_{0.40}\text{Zn}_{0.60}\text{O}$  photodetector has been fabricated and its response characteristics are studied.

## Experiment

The sample used in this study was grown by the radio frequency (rf) magnetron sputtering technique. A  $\text{Mg}_{0.18}\text{Zn}_{0.82}\text{O}$  target was prepared by a sintering mixture of 99.99% pure MgO and ZnO powders at 1273 K for 10 h in ambient air. The sputtering chamber was pumped down to a high vacuum of  $5.0 \times 10^{-4}$  Pa by a turbo molecular pump. Ultrapure (5 N) Ar and N<sub>2</sub> gases were introduced into the sputtering chamber through a set of mass flow controllers with flow rates of 22.5 sccm (standard cubic centimeters per minute). The working pressure in the chamber was kept at 1 Pa with an rf power of 100 W, and the

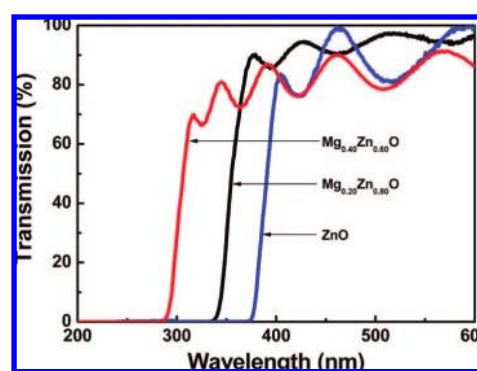


**Figure 1.** Transmission spectra of  $\text{Mg}_{0.40}\text{Zn}_{0.60}\text{O}$ ,  $\text{Mg}_{0.20}\text{Zn}_{0.80}\text{O}$ , and ZnO thin films grown on quartz substrates.

substrate temperature was controlled at about 673 K during the sputtering process. To improve the crystal quality, the films were annealed at 873 K for 10 min under  $1.0 \times 10^{-4}$  Pa in a vacuum chamber after sputtering. The Mg composition in the films was measured by energy-dispersive spectroscopy (EDS) and found to be  $\text{Mg}_{0.40}\text{Zn}_{0.60}\text{O}$ . The difference between the Mg percentage in the target and that in the film was attributed to the high vapor pressure of Zn. It should be noted that no phase separation was observed after annealing, and the absorption edge blue-shifted obviously, which is explained in our previous paper.<sup>13</sup>

## Results and Discussion

The optical transmission spectra were recorded using a Shimadzu UV-3101PC scanning spectrophotometer. Shown in Figure 1 is the transmission spectrum of the  $\text{Mg}_{0.40}\text{Zn}_{0.60}\text{O}$  thin film. The spectra of  $\text{Mg}_{0.20}\text{Zn}_{0.80}\text{O}$  and ZnO are also presented for comparison. The transmission spectra of all three films have more than 80% transmission in the visible region. Clearly, the absorption edge of the  $\text{Mg}_{0.40}\text{Zn}_{0.60}\text{O}$  thin film is at about 300 nm. It is interesting to note that all three samples exhibit a sharp absorption edge, whereas in the earlier reports a broadening in the absorption edge is normally observed at higher Mg composition and is usually attributed to the Mg segregation from the lattice site of  $\text{Mg}_x\text{Zn}_{1-x}\text{O}$  thin films.<sup>14,15</sup> In this work, no such broadening is observed in the sputtered  $\text{Mg}_{0.40}\text{Zn}_{0.60}\text{O}$  thin film.

The structural properties of the  $\text{Mg}_x\text{Zn}_{1-x}\text{O}$  thin films were characterized by X-ray diffraction (XRD) using a D/max-RA

\* To whom correspondence should be addressed. E-mail: zhangjiy53@yahoo.com.cn.

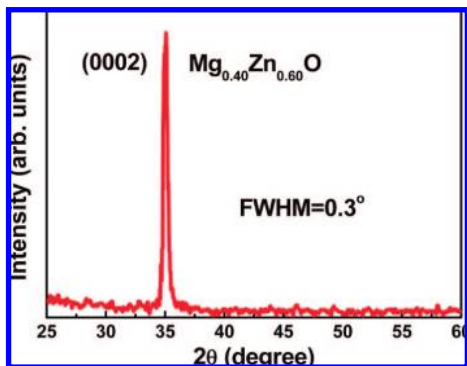


**Figure 2.** XRD pattern of the  $\text{Mg}_{0.40}\text{Zn}_{0.60}\text{O}$  thin film prepared on quartz by the rf magnetron sputtering technique.

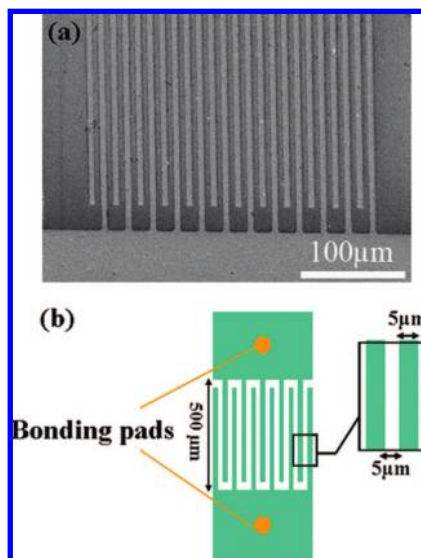


**Figure 3.** (a) Optical microscope top view of the MSM structured photodetector showing interdigitated electrodes. (b) Schematic illustration of the interdigitated electrodes including the values of the finger width and the spacing.

X-ray spectrometer (Rigaku) with  $\text{Cu K}\alpha$  radiation of 0.154 nm. Figure 2 shows the XRD pattern of the  $\text{Mg}_{0.40}\text{Zn}_{0.60}\text{O}$  thin film grown on a quartz substrate after annealing. Only a (0002) diffraction peak can be observed, indicating that the film is hexagonally structured and highly  $c$ -axis oriented.<sup>16</sup> The peak is Gaussian symmetrical with a full width at half-maximum (fwhm) of  $0.3^\circ$ . The film thickness was 550 nm after deposition and 500 nm after annealing. The mean size of the  $\text{Mg}_{0.40}\text{Zn}_{0.60}\text{O}$  crystallites was about 50 nm. It should be noted that only a few groups have obtained single-phased  $\text{Mg}_x\text{Zn}_{1-x}\text{O}$  alloys with Mg concentration larger than 40%.<sup>12</sup>

The metal–semiconductor–metal (MSM) structure was fabricated on the  $\text{Mg}_{0.40}\text{Zn}_{0.60}\text{O}$  thin film using an interdigitated electrode mask set, an image of which is shown by the optical microscope photograph in Figure 3a. The electrode fingers are 5  $\mu\text{m}$  wide and 500  $\mu\text{m}$  long with a 5  $\mu\text{m}$  spacing gap. A schematic illustration of the interdigitated electrodes is shown in Figure 3b. A 200 nm thick Au layer was deposited using the vacuum evaporation method with a growth rate of approximately 50 nm/min. Au was chosen as the Schottky metal contact because of its comparatively high work function ( $\Phi = 5.1$  eV), as well as the encouraging results reported in Au/ZnO Schottky diodes previously. The MSM electrodes were then fined by conventional UV photolithography and wet etching.

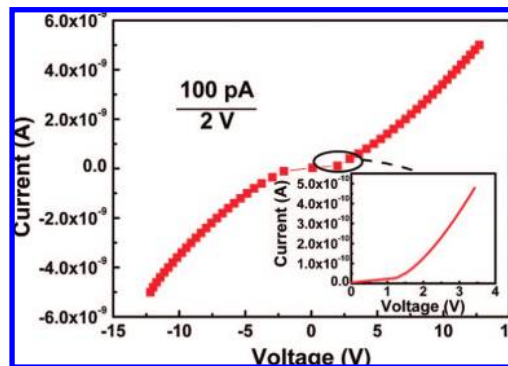


**Figure 4.**  $I$ – $V$  characteristic of the  $\text{Mg}_{0.40}\text{Zn}_{0.60}\text{O}$  MSM Schottky photodetector in the dark. The inset shows a magnified illustration of the  $I$ – $V$  curve.

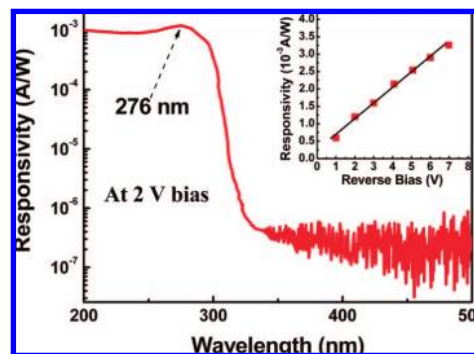


**Figure 5.** Spectral response of the  $\text{Mg}_{0.40}\text{Zn}_{0.60}\text{O}$  photodetector biased at 2 V. The inset shows the peak responsivity at 276 nm as a function of the bias voltage.

The dark current measurements were obtained under the van der Pauw configuration by a Hall effect measurement system at room temperature. As shown in Figure 4, a very low dark current of  $\sim 100$  pA at a bias of 2 V is obtained, which is far smaller than the previous published data.<sup>10,17</sup> The fact is that the device presented a very low dark current due to the wide band gap and Schottky barrier height. We note that the Schottky barrier exhibited no degradation even when biased beyond 15 V for extended periods of time.

The spectral responsivity was measured with a standard lock-in amplifier, where a 150 W Xe lamp was used. Figure 5 shows the spectral responsivity of the Schottky barrier  $\text{Mg}_{0.40}\text{Zn}_{0.60}\text{O}$  photodetector at a bias of 2 V. The peak response is 0.0012 A/W at 276 nm. The cutoff wavelength is at 295 nm, which is in agreement with the absorption edge shown in Figure 1. The ultraviolet-to-visible rejection [ $R(276 \text{ nm})/R(400 \text{ nm})$ ] is about 4 orders of magnitude. The inset of Figure 5 shows the responsivity as a function of the bias voltage. A linear relationship is obtained, indicating no carrier mobility saturation or sweep-out effect happens at up to 7 V bias. The noise equivalent power (NEP) can be calculated by  $\text{NEP} = (4k_B T / R_{\text{dark}} + 2qI_{\text{dark}})^{1/2} \Delta f^{1/2} / R$ , where  $R_{\text{dark}}$  refers to the equivalent resistance obtained from the slope of the dark current  $I$ – $V$  curve at the bias point,  $I_{\text{dark}}$  is the dark current at the bias point,  $T$  is the temperature,  $\Delta f$  is the bandwidth of the measurement, and  $R$  is the measured responsivity. The normalized detectivity ( $D^*$ ) can then be determined by  $D^* = (A\Delta f)^{1/2} / (\text{NEP})$ , where  $A$  is the device area. With 2 V applied bias, a maximum  $D^*$  of  $1.37 \times 10^{12}$  ( $\text{cm Hz}^{1/2})/\text{W}$  at 276 nm is obtained. It should be noted that the detectivity measured from our  $\text{Mg}_{0.40}\text{Zn}_{0.60}\text{O}$  UV

detector is higher than those observed from ZnO and GaN-based MSM photodetectors with a similar structure.<sup>17,18</sup>

### Conclusions

In summary, we have demonstrated MSM structured Schottky barrier  $\text{Mg}_{0.40}\text{Zn}_{0.60}\text{O}$  photodetectors. The photodetector shows a peak responsivity at 276 nm, and the corresponding detectivity is  $1.1 \times 10^{12}$  ( $\text{cm Hz}^{1/2}/\text{W}$ ). A sharp cutoff wavelength is at 295 nm, and the ultraviolet-to-visible rejection is about 4 orders of magnitude. The dark current is only about 100 pA at 2 V bias. We believe that these results represent a significant step toward achieving practical solid-state UV photodetectors based on the  $\text{Mg}_x\text{Zn}_{1-x}\text{O}$  material system.

**Acknowledgment.** This work is supported by the Key Project of the National Natural Science Foundation of China under Grant Nos. 60336020 and 50532050 and the “973” program under Grant Nos. 2008CB317105 and 2006CB604906.

### References

- (1) Razeghi, M.; Rogalski, A. *J. Appl. Phys.* **1996**, *79*, 7433.
- (2) Ulmer, M. P.; Razeghi, M.; Bigan, E. *Proc. SPIE—Int. Soc. Opt. Eng.* **1995**, *2397*, 210.
- (3) Rogalski, A.; Razeghi, M. *Opto-Electron. Rev.* **1996**, *4*, 13.
- (4) Streltsov, A. M.; Moll, K. D.; Gaeta, A. L.; Kung, P.; Walker, M. D.; Razeghi, M. *Appl. Phys. Lett.* **1999**, *75*, 3378.
- (5) McKinley, A. F.; Diffey, B. L. *CIE J.* **1987**, *6*, 17.
- (6) Narayan, J.; Sharma, A. K.; Kvit, A.; Jin, C.; Muth, J. F.; Holland, O. W. *Solid State Commun.* **2002**, *121*, 9.
- (7) Choopun, S.; Vispute, R. D.; Yang, W.; Sharma, R. P.; Venkatesan, T.; Shen, H. *Appl. Phys. Lett.* **2002**, *80*, 1529.
- (8) Auret, F. D.; Goodman, S. A.; Hayes, M.; Legodi, M. J.; van Laarhoven, H. A.; Look, D. C. *Appl. Phys. Lett.* **2001**, *79*, 3074.
- (9) Hullavarad, S. S.; Dhar, S.; Varughese, B.; Takeuchi, I.; Venkatesan, T.; Vispute, R. D. *J. Vac. Sci. Technol.* **2005**, *A23*, 982.
- (10) Liu, K. W.; Zhang, J. Y.; Ma, J. G.; Jiang, D. Y.; Lu, Y. M.; Yao, B.; Li, B. H.; Zhao, D. X.; Zhang, Z. Z.; Shen, D. Z. *J. Phys. D: Appl. Phys.* **2007**, *40*, 2765.
- (11) Yang, W.; Hullavarad, S. S.; Nagaraj, B.; Takeuchi, I.; Sharma, R. P.; Venkatesan, T.; Vispute, R. D.; Shen, H. *Appl. Phys. Lett.* **2003**, *82*, 3424.
- (12) Kumar, S.; Gupte, V.; Sreenivas, K. *J. Phys.: Condens. Matter* **2006**, *18*, 3343.
- (13) Jiang, D. Y.; Shen, D. Z.; Liu, K. W.; Shan, C. X.; Zhao, Y. M.; Yang, T.; Yao, B.; Lu, Y. M.; Zhang, J. Y. *Semicond. Sci. Technol.* **2008**, *23*, 035002.
- (14) Minemoto, T.; Negami, T.; Nishiwaki, S.; Takakura, H.; Hamakawa, Y. *Thin Solid Films* **2000**, *372*, 173.
- (15) Sharma, A. K.; Narayan, J.; Muth, J. F.; Teng, C. W.; Jin, C.; Kvit, A.; Kolbas, R. M.; Holland, Q. W. *Appl. Phys. Lett.* **1999**, *75*, 3327.
- (16) JCPDS card 80-0075.
- (17) Liu, K. W.; Shen, D. Z.; Shan, C. X.; Zhang, J. Y.; Yao, B.; Zhao, D. X.; Lu, Y. M.; Fan, X. W. *Appl. Phys. Lett.* **2007**, *91*, 201106.
- (18) Wang, C. K.; Chang, S. J.; Su, Y. K.; Chiou, Y. Z.; Chang, C. S.; Lin, T. K.; Liu, H. L.; Tang, J. J. *Semicond. Sci. Technol.* **2005**, *20*, 485.

CG800706M